

An Innovative One-Step Method to Produce Membranes with a Pore Size Gradient

Elena Inzerillo*, Valerio Brucato, Gaetano Burriesci, Francesco Carfi Pavia, Tommaso Ingrassia

Department of Engineering, University of Palermo, Viale delle Scienze, 90128 Palermo, Italy
elena.inzerillo@unipa.it

The fabrication of porous scaffolds with continuous pore size gradients is growing in interest in tissue engineering, as graded architectures better mimic the structural heterogeneity of native interfacial tissues. Conventional strategies based on monolayer scaffolds fail to reproduce this heterogeneity, while multilayer constructs introduce interfaces that do not ensure continuous transitions in structural and mechanical properties. Although most gradient fabrication approaches rely on multistep or post-processing techniques, limited attention has been focused to procedures allowing to obtain directly the final scaffold. Thermally induced phase separation is a versatile method for regulating pore morphology in scaffold by controlling the thermal history. This work investigates a TIPS-based strategy to generate continuous pore size gradients by tailoring heat transfer directionality. Poly-L-lactic acid scaffolds were produced using two process configurations differing in the presence or absence of thermal insulation and analysed using a combined experimental and numerical approach. Scaffold morphology was characterised by scanning electron microscopy, while thermal transient simulations were performed to investigate temperature evolution during phase separation and freezing. The analysis highlights differences in cooling behaviour between the two configurations, correlating these with variations in pore size distribution across the scaffold thickness. The results demonstrated that it is possible to obtain scaffold with a pore size gradient through a one-step TIPS procedure.

1. Introduction

Several native tissues exhibit gradual transitions in structural and functional properties. Interfacial tissues, such as cartilage-bone and tendon-bone junctions, are characterized by soft-hard interfaces where graded architectures support physiological load transfer and tissue integration (Ansari et al., 2019). Tissue engineering (TE) aims to recreate microenvironments that mimic the structural and cellular complexity of native tissues. However, replicating graded features represents a central challenge, as spatial gradients regulate cellular behaviours, tissue organization, nutrient diffusion and angiogenesis (Conoscenti et al., 2017). Several studies aiming to recreate interfacial tissue microenvironments are based on monolayer and multilayer scaffold designs. Monolayer scaffolds exhibit uniform porosity and structural features throughout their thickness and, although they support cell growth, they fail to reproduce the heterogeneity of native interfacial tissues. To overcome these limitations, multilayer scaffolds composed of discrete layers have been developed. However, these constructs do not ensure a continuous transition in structural and mechanical properties across the scaffold thickness (Niu et al., 2023). For this reason, scaffolds with pore size gradients are increasingly explored as a strategy to achieve biomimetic scaffold architectures. These constructs are based on a single continuous matrix with spatially graded properties, enabling smooth transitions that avoid discrete layers stratification and reduce interfacial instability. Moreover, the gradual variation of structural features enhances fluid and nutrient diffusion, supporting vascular ingrowth and providing appropriate mechanical support (Chen et al., 2023). Scaffold pore size and porosity play a key role in regulating cell behaviour, influencing cell adhesion, migration and phenotype expression, as well as nutrient diffusion and degradation kinetics (Rigogliuso et al., 2012). Among scaffold fabrication techniques, thermally induced phase separation (TIPS) provides a versatile approach for tailoring porous architectures through several processing parameters. In particular, thermal history during processing

plays a key role in determining pore morphology and spatial distribution, allowing controlled modulation of pore size and interconnectivity (Chen et al., 2010). Despite the growing interest in pore size gradient scaffold, most production techniques rely on complex multistep processes or post-processing strategies to generate this spatial variation. Few studies have been focused to directional control of the cooling process during TIPS to directly generate continuous pore size gradients. In this context, the present work investigates a one-step TIPS-based approach to produce scaffolds with a controlled pore size gradient by tailoring the direction of heat transfer during the process. Specifically, the study investigates how the presence of thermal insulation influences heat transfer directionality and, consequently, the spatial distribution of pore size across the scaffold thickness. By controlling thermal conditions, the proposed strategy aims to enable the formation of continuous pore size gradients without post-processing steps.

2. Materials and method

2.1 Thermal transient analysis (MATLAB)

Thermal transient analyses were performed using the Partial Differential Equations (PDE) Toolbox in MATLAB to model heat transfer during the TIPS process and evaluate temperature evolution during cooling. Heat transfer was assumed to be conduction-dominated, and the transient heat conduction equation (Eq. 1) was solved:

$$\rho c_p \frac{\partial T}{\partial t} = \nabla(k \nabla T) \quad (1)$$

where ρ is the density, c_p the specific heat capacity, k the thermal conductivity and T the temperature. The thermal properties of the fused-quartz sample holder and the insulating layer were assumed constant, while temperature-dependent properties were assigned to the polymeric solution based on mixing rules. For the first thermostatic bath, the initial temperatures of the polymeric solution and the sample holder were set to 60 °C, while the insulating layer was set to 25 °C (room temperature). A boundary temperature of 30 °C was imposed on the external faces exposed to the bath. The transient simulation was carried out for 45 min, and the temperature profiles were extracted at regular time intervals from the mid-height plane of the model. For the second thermostatic bath, the initial temperature of all domains was set to 30 °C, with a boundary temperature of -20 °C imposed on the external faces exposed to the cooling bath. The thermal transient was simulated for 30 min, and temperature profiles were extracted along the same spatial directions. Transient thermal analysis was also performed in a restricted time interval corresponding to the solidification stage of the polymeric solution. Based on thermodynamic data for the water-dioxane system, the onset of solidification occurs at approximately 4 °C (Goates & Sullivan, 1958). Considering the low PLLA concentration in the ternary solution (4% w/v), its contribution to the freezing point can be considered negligible (J. S. Chen et al., 2010). Therefore, the freezing temperature of the ternary system was approximated to that of the binary water-dioxane system. Within this interval, temperature profiles were extracted every 20 s along the full thickness of the polymeric solution, from the exposed face to the opposite, in both the reference and modified process configurations.

2.2 Materials

Poly-L-lactic acid (PLLA, Resomer® L 209 S, Evonik Industries, Essen, Germany), 1,4-dioxane (Sigma-Aldrich, Munich, Germany) and ultrapure water were used for scaffold preparation.

2.3 Scaffold Fabrication via thermally induced phase separation (TIPS)

A ternary solution of PLLA, 1,4-dioxane and water (4% w/w PLLA; 87/13 w/w solvent-antisolvent ratio) was prepared following the protocol reported by (La Carrubba et al., 2008). First, PLLA was dissolved in 1,4-dioxane under magnetic stirring at 220 °C until complete dissolution was achieved. Then, water was added dropwise to the PLLA/1,4-dioxane solution at 45 °C under continuous stirring, and the mixture was heated to obtain a homogeneous ternary solution.

Finally, the resulting solution was maintained at 60 °C before further processing.

PLLA scaffolds were fabricated via TIPS using a protocol adapted from (Carfi Pavia et al., 2008). The polymeric solution was cast into a preheated parallelepipedal fused-quartz sample holder at 60 °C and then immersed in a thermostatic bath at 30 °C for 45 min to induce phase separation. The system was then transferred to a second thermostatic bath at -20 °C for 30 min to promote the controlled freezing of the structure. After solidification, the frozen structure was removed from the sample holder, washed in water to remove residual solvent and then dried at 60 °C. Two different process configurations were investigated. In the reference configuration, the sample holder was directly immersed in the thermostatic baths. In the modified configuration, a 5 mm expanded polyethylene insulating layer was applied to three sides of the sample holder during both thermal steps to impose a preferential direction of heat transfer.

2.4 Morphological characterization with scanning electron microscopy (SEM)

Scaffold morphology was analysed using Scanning Electron Microscopy (SEM) with a Philips Quanta 200 F microscope operated at an accelerating voltage of 10 kV. Parallelepipedal scaffolds were sectioned to obtain a cross section with a thickness of approximately 2 mm. Each sample was then sputter-coated with a thin gold layer using a ScanCoat Six sputter coater (Edwards, Irvine, CA, USA) under vacuum and an argon atmosphere for 120 s to ensure surface conductivity. Pore size measurements were performed on SEM images of both the reference and modified configuration using ImageJ software. Measurements were taken within the first 1.5 cm from the two opposite borders of each scaffold and a total of 30 pores per region were analyzed. To assess statistical differences between pore diameters measured in the small-pore and large-pore regions of the scaffold, a two-sample t-test was performed.

3. Results and discussion

3.1 Model geometry

The model geometry of the reference configuration contained two domains: the polymer solution and the sample holder. In the modified configuration, a third domain representing the insulating layer was added and positioned to cover three sides of the sample holder. Figure 1 shows a schematic representation of the domains in both configurations.

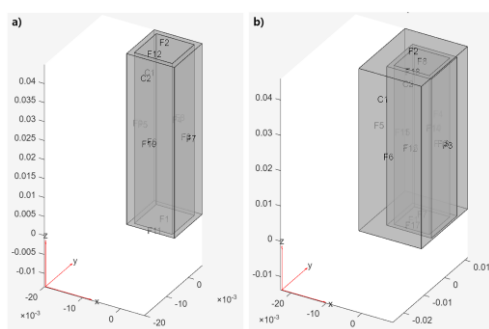


Figure 1: Computational domains used for thermal transient analysis: (a) reference configuration without thermal insulation; (b) modified configuration with an insulating layer applied to three sides of the sample holder.

A Cartesian reference system was defined with the origin located at the geometric centre of the polymeric solution. Temperature profiles were extracted along three spatial directions in both configurations. As shown in Figure 2, the +X direction was defined as normal to the face directly exposed to the thermostatic bath, the -X direction was normal to the opposite, insulated side and the Y direction was normal to the lateral face of the sample holder.

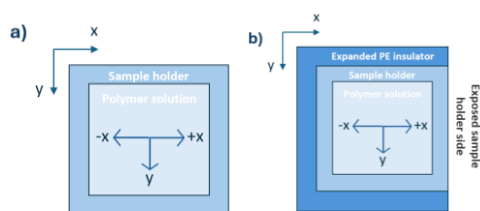


Figure 2: Schematic representation of the system (above view) in the (a) reference configuration and (b) modified configuration

3.2 Thermal transient analysis (MATLAB)

During the first thermostatic bath (60 °C → 30 °C), the system's thermal behaviour was analysed to assess the influence of thermal insulation on temperature evolution over time. In both the reference and modified configurations, the polymeric solution exhibited a rapid and homogeneous cooling behaviour, achieving the thermal equilibrium with the 30 °C bath without developing spatial temperature gradients. The insulating layer had a small effect on the cooling kinetics, resulting in a delay of approximately 5 min in reaching the bath

temperature. However, given that the total residence time in the first thermostatic bath is 45 min, it can be assumed that this delay should not affect the overall thermal uniformity of the system. These results suggest that phase separation during the first cooling step under carried out in homogeneous thermal conditions and does not contribute to the development of directional thermal gradients.

Figure 3 reports the simulated temperature profiles during the second thermostatic bath (30 °C → -20 °C) for both process configurations. For each spatial direction, temperature profiles obtained in the reference configuration (Figure 3a) exhibit a symmetric behaviour, indicating an isotropic heat transfer process. In contrast, a markedly different thermal response is observed in the modified configuration (Figure 3b).

Temperature profiles along the +X direction show a faster temperature decrease compared to the -X direction, where the presence of the insulating layer slows heat transfer.

As a result, a pronounced temperature gradient should develop across X direction. Temperature profiles along the Y direction remain uniform across the sample length, suggesting the absence of significant lateral thermal gradients.

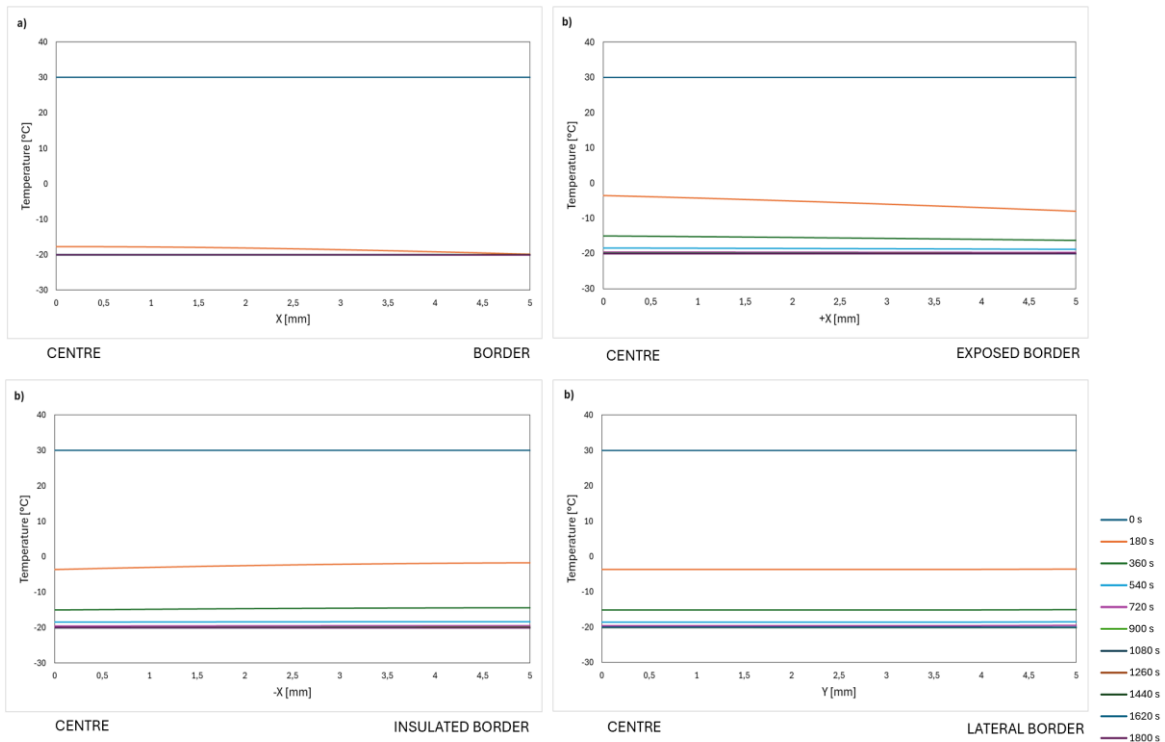


Figure 3: Temperature profiles during the second thermostatic bath (-20 °C) for (a) reference configuration and (b) modified configuration

Figure 4 reports the simulated temperature profiles during the early stages of scaffold freezing, focusing on the first 140 s of the second thermostatic bath. The isothermal line indicates the estimated freezing temperature of the polymeric solution (~ 4 °C).

In the reference configuration (Figure 4a), the temperature profiles exhibit symmetrical behaviour with respect to the centre of the sample.

The freezing threshold is reached earlier in the outer regions of the sample and progressively later towards the centre, resulting in a symmetric, centripetal solidification pattern characterized by a parabolic temperature distribution across the thickness. In contrast, the modified configuration (Figure 4b) exhibits markedly different thermal evolution behaviour.

The freezing threshold is first reached near the face directly exposed to the cooling bath and progressively advances towards the insulated face.

This phenomenon generates a cooling front propagation along the X direction. Consequently, in this case the solution does not cool symmetrically, as in reference configuration, but it cools following a preferential direction, giving rise to temperature gradient along X axis, which should lead in a difference in pore size in the resulting scaffolds.

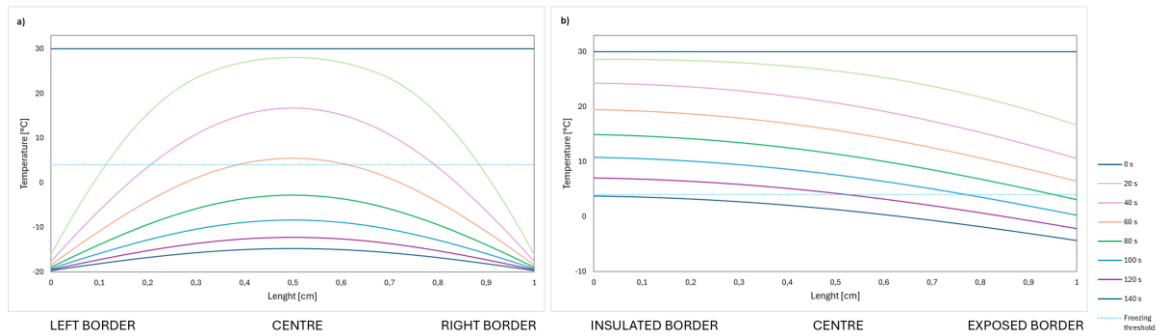


Figure 4: Temperature profiles along the scaffold thickness during the early freezing stage (first 140 s of the second thermostatic bath) for (a) the reference configuration and (b) the modified configuration.

3.3 Morphological characterization with Scanning Electron Microscopy (SEM)

In the Figure 5 is reported the comparison of scaffold morphologies obtained from the reference and the modified process configurations. SEM images of the reference configuration (Figure 5a) exhibit a region of smaller pores at the sample borders, followed by a gradual increase in pore size toward the centre of the scaffold. This morphology reflects a symmetric cooling process, in which, as shown above, heat transfer occurs simultaneously from all external faces towards the core of the sample. In contrast, SEM images of the modified configuration (Figure 5b) show a markedly different pore size distribution. The exposed side of the scaffold exhibits a region of smaller pores, while pore size progressively increases towards the opposite side. Pore size measurements performed on the modified configuration confirm this trend (Table 1), showing an increase in average pore diameter from $134.63 \pm 20.73 \mu\text{m}$ at the exposed border to $189.76 \pm 38.77 \mu\text{m}$ towards the insulated side. Statistical analysis using a two-sample t-test confirmed that the difference between the two pore populations is statistically significant ($p < 0.001$). Hence, the modified configuration, according to the simulations, gives rise to a continuous pore size gradient along the scaffold thickness.

Table 1: Average pore size measurements

Configuration	Scaffold region	Average pore size [μm]	p value
Reference configuration	Left border	130.33 ± 37.72	> 0.05
	Right border	137 ± 31.32	
Modified configuration	Exposed border	134.63 ± 20.73	< 0.001
	Insulated border	189.76 ± 38.77	

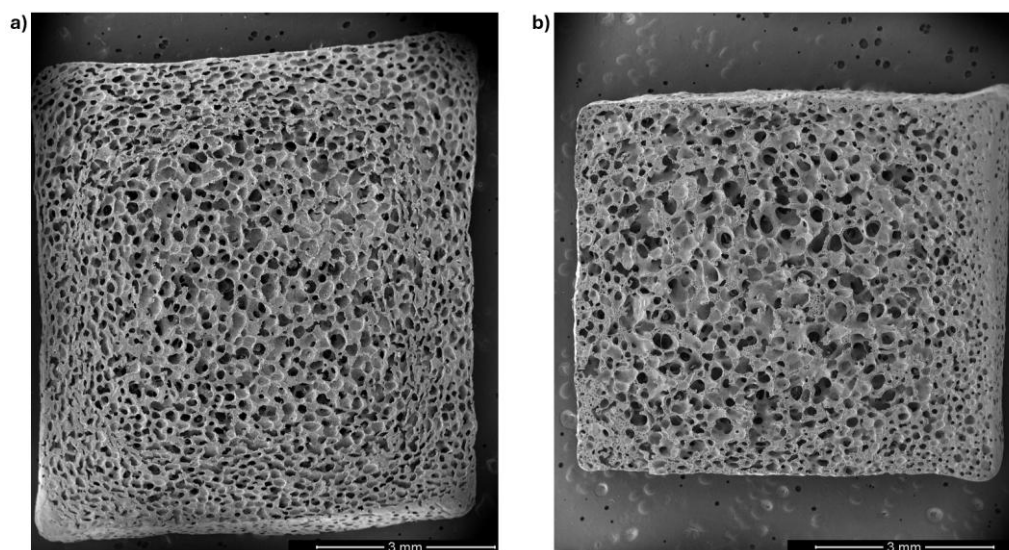


Figure 5: SEM images of scaffold from the (a) reference configuration and (b) modified configuration

4. Conclusions

This study compared two TIPS-based process configurations to investigate the role of heat transfer control on the scaffold morphology and its pore size distribution. Without thermal insulation, the results demonstrated that heat transfer occurs symmetrically from all external surfaces, leading to a centripetal cooling process and non-directional pore size distributions. In contrast, the introduction of a thermal insulating layer influenced the heat transfer directionality, promoting an asymmetric and progressive cooling front across the scaffold thickness and enabling the formation of a continuous pore size gradient. Experimentally, pore size increased from approximately 135 μm at the exposed border to about 190 μm towards the insulated side of the scaffold. The proposed one-step TIPS approach is an effective strategy for generating gradient porous architecture, eliminating the need for post-processing steps. Combined experimental and numerical analyses highlighted the central role of thermal history and controlled cooling direction in governing solidification dynamics and final scaffold morphology. These findings suggest that directional thermal control during TIPS could be employed as a versatile method for engineering continuous pore size gradients.

Nomenclature

ρ – density, kg/m^3
 c_p – specific heat capacity, $\text{J}/(\text{kg}\cdot\text{K})$
 k – thermal conductivity, $\text{W}/(\text{m}\cdot\text{K})$
 T – temperature, $^\circ\text{C}$
 t – time, s
 X, Y – spatial coordinates, m

Acknowledgments

E.I. would like to thank Dott. Dario Davì for his valuable contribution to the transient thermal analyses.

References

- Ansari, S., Khorshidi, S., & Karkhaneh, A. (2019). Engineering of gradient osteochondral tissue: From nature to lab. *Acta Biomaterialia*, 87, 41–54. <https://doi.org/10.1016/j.actbio.2019.01.071>
- Carfi Pavia, F., La Carrubba, V., Piccarolo, S., & Brucato, V. (2008). Polymeric scaffolds prepared via thermally induced phase separation: Tuning of structure and morphology. *Journal of Biomedical Materials Research Part A*, 86A(2), 459–466. <https://doi.org/10.1002/jbm.a.31621>
- Chen, J. S., Tu, S. L., & Tsay, R. Y. (2010). A morphological study of porous polylactide scaffolds prepared by thermally induced phase separation. *Journal of the Taiwan Institute of Chemical Engineers*, 41(2), 229–238. <https://doi.org/10.1016/j.jtice.2009.08.008>
- Chen, L., Wei, L., Su, X., Qin, L., Xu, Z., Huang, X., Chen, H., & Hu, N. (2023). Preparation and Characterization of Biomimetic Functional Scaffold with Gradient Structure for Osteochondral Defect Repair. *Bioengineering*, 10(2), 213. <https://doi.org/10.3390/bioengineering10020213>
- Conoscenti, G., Schneider, T., Stoelzel, K., Carfi Pavia, F., Brucato, V., Goegele, C., La Carrubba, V., & Schulze-Tanzil, G. (2017). PLLA scaffolds produced by thermally induced phase separation (TIPS) allow human chondrocyte growth and extracellular matrix formation dependent on pore size. *Materials Science and Engineering: C*, 80, 449–459. <https://doi.org/10.1016/j.msec.2017.06.011>
- Goates, J. R., & Sullivan, R. J. (1958). Thermodynamic Properties of the System Water-p-Dioxane. *The Journal of Physical Chemistry*, 62(2), 188–190. <https://doi.org/10.1021/j150560a011>
- La Carrubba, V., Carfi Pavia, F., Brucato, V., & Piccarolo, S. (2008). PLLA/PLA scaffolds prepared via Thermally Induced Phase Separation (TIPS): Tuning of properties and biodegradability. *International Journal of Material Forming*, 1(S1), 619–622. <https://doi.org/10.1007/s12289-008-0332-5>
- Niu, X., Li, N., Du, Z., & Li, X. (2023). Integrated gradient tissue-engineered osteochondral scaffolds: Challenges, current efforts and future perspectives. *Bioactive Materials*, 20, 574–597. <https://doi.org/10.1016/j.bioactmat.2022.06.011>
- Rigogliuso, S., Carfi Pavia, F., Brucato, V., La Carrubba, V., Favia, P., Intranuovo, F., Gristina, R., & Ghersi, G. (2012). Use of Modified 3D Scaffolds to Improve Cell Adhesion and Drive Desired Cell Responses. *Chemical Engineering Transactions*.